Harmonic Orbital Resonances and Orbital Long-Range Order of the TRAPPIST-1 Exoplanetary System

Felix Scholkmann

Research Office for Complex Physical and Biological Systems (ROCoS),
Mutschellenstr. 179, 8038 Zurich, Switzerland. E-mail: felix.scholkmann@gmail.com

Recently, seven exoplanets orbiting the ultra-cool dwarf star TRAPPIST-1 were reported. The present paper explores whether (i) the sequence of semi-major axis values of the planets shows a long-range order, and whether (ii) the values can be described by harmonic orbital resonances. The analysis showed that orbits of the planets follow (i) a long-range order, and (ii) a quantization in accordance with harmonic orbital resonances. The study supports the view that planetary systems are best viewed as self-organizing systems with attractor states of the planet orbits being related to resonance effects.

1 Introduction

A paper [1] was recently published on the discovery and description of an extrasolar planetary system with seven planets (TRAPPIST-1b, c, d, e, f, g and h) orbiting an ultra-cool dwarf star (TRAPPIST-1, 2MASS J23062928-0502285; apparent magnitude: $V = 18.80$) in the constellation Aquarius ($RA = 23^h\,06^m\,29.28^s$, dec $= -05°\,02'\,28.5''$).

This discovery was the result of an intensive observation program using space- and earth-based telescopes comprising the TRAPPIST (TRansiting Planets and PlanestIsimals Small Telescope) North system (Chile), the TRAPPIST-North telescope (Morocco), the Himalayan Chandra Telescope (India), the Very Large Telescope (Chile), the UK Infrared Telescope (Hawaii), the Spitzer Space Telescope, the William Herschel and Liverpool telescopes (La Palma, Spain), as well as the South African Astronomical Observatory telescope [1, 2].

The orbital parameters of the TRAPPIST-1 planetary system exhibit a non-random behaviour, i.e., "the six inner planets form the longest known near-resonant chain of exoplanets, with the ratios of the orbital periods (P) P_c/P_b, P_d/P_c, P_e/P_d, P_f/P_e and P_g/P_f being close to the ratios of small integers, namely 8/5, 5/3, 3/2, 3/2 and 4/3, respectively", as noted in the recent *Nature* publication [1]. A property that is associated with an *orbital resonance*, or a mean-motion orbital resonance, in particular. Other examples of planetary systems where the *orbital periods* are in a specific resonance-like relationship include the exoplanetary systems Kepler-223 [3], Kepler-80 [4], GJ 876 [5] and HD 82943 [6]. If the orbital *periods* show this resonance phenomenon, then also the orbital *spacing* of a planetary system follows the same pattern – a direct consequence of Kepler's third law linking the orbital spacing (given as the semi-major axis, (a)) with the period of an planet orbiting a star, $P^2 \propto a^3$, leading to the relationships $a \propto P^{2/3}$ and $P \propto a^{3/2}$.

The orbital resonances can be analysed by examining the orbital spacings locally and separately, or by analysing the whole planetary system orbital spacing *in toto*. Foundational work on this second approach was conducted by J. Bohr and

K. Olsen [9, 10] who showed that the orbital spacing of the planets of our solar system follows long-range order on a logarithmic scale, i.e., the logarithmic positions of the planets are correlated and follow a periodic pattern (a kind of "quantization") [9]. This long-range order of the orbital spacing was also detected in the exoplanetary system HD 10180 [10]. Stimulated by this work, I showed in 2013 that the orbital spacing of the exoplanetary system Kepler-62 exhibits a long-range order too and I predicted an additional planet (which has not been detected yet, however) based on this analysis [7].

The discovery of the TRAPPIST-1 planetary system [1] triggered the question of whether the orbital spacing of this system also follows a long-range order, and how the orbital structure of the planetary system can be described based on approach of orbital resonances. The aim of the present work was therefore to investigate these two asepcts in detail.

2 Materials and methods

2.1 Data

The parameter values of the TRAPPIST-1's exoplanets were obtained from Gillon et al. [1]. In the present work, two parameters were selected for analysis: the semi-major axis (a) and the radius (r) of each planet (see Table 1).

2.2 Analysis of the orbital long-range order

To analyse the TRAPPIST-1 system, the same approach as already employed for the previously published analysis of the Kepler-62 system [7] was used. In particular, the semi-major axis values a (given in units of 10^6 km) of each exoplanet were first divided by 10^6 km, then logarithmized ($\hat{a}_i = \ln(a_i/10^6$ km$)$) and according to these values a multi-modal probability distribution function (PDF) $p(\hat{a})$ was calculated by

$$p(\hat{a}) = \sum_{i=1}^{N} \alpha_i\, e^{-\beta}, \qquad (1)$$

Planet	i	a [AU]	a [km]	r [$R_\oplus$]	r [km]	$\hat{a}$
b	1	0.01111 ± 0.00034	$1.6621 \times 10^6 \pm 5.0864 \times 10^4$	1.086 ± 0.035	6926.508 ± 223.23	0.5081
c	2	0.01521 ± 0.00047	$2.2754 \times 10^6 \pm 7.0312 \times 10^4$	1.056 ± 0.035	6735.168 ± 223.23	0.8222
d	3	$0.02144^{+0.00066}_{-0.00063}$	$3.2074 \times 10^6\ ^{+9.8736 \times 10^4}_{-9.4248 \times 10^4}$	0.772 ± 0.03	4923.816 ± 191.34	1.1655
e	4	$0.02817^{+0.00083}_{-0.00087}$	$4.2142 \times 10^6\ ^{+1.2417 \times 10^4}_{-1.3015 \times 10^4}$	0.918 ± 0.039	5855.004 ± 248.742	1.4385
f	5	0.0371 ± 0.0011	$5.5502 \times 10^6 \pm 1.6456 \times 10^5$	1.045 ± 0.038	6665.01 ± 242.364	1.7138
g	6	0.0451 ± 0.0014	$6.7470 \times 10^6 \pm 2.0944 \times 10^5$	1.127 ± 0.041	7188.006 ± 261.498	1.9091
h	7	$0.063^{+0.027}_{-0.013}$	$9.4248 \times 10^6\ ^{+4.0392 \times 10^6}_{-1.9448 \times 10^6}$	0.755 ± 0.034	4815.39 ± 216.852	2.2433

Table 1: TRAPPIST-1 system parameters according to [1]. i: planet number counting outwardly from the star TRAPPIST-1, a: semi-major axis, r: radius of the planet, $\hat{a}_i = \ln(a_i/10^6 \text{ km})$, a and r are given in two different units ([AU], [km]) and ([$R_\oplus$], [km]), respectively.

with $N = 7$ (i.e., the maximum number of planets of the TRAPPIST-1 system) and β given as

$$\beta = \frac{j - \hat{a}_i}{w_p / 2 \sqrt{2 \ln(2)}}, \qquad (2)$$

for $j = 1, 1.01, 1.02, \ldots, 3$, with w_p the width (i.e., the full-width-at-half-maximum) of each Gaussian peak of the PDF, and α_i a scale factor. This approach was first introduced by Bohr and Olsen [9]. The scale factor α in equation (1) defines the magnitude of each peak of the PDF and was assigned to the radius of the specific planet ($\alpha_i = r_i$). With this the size of the planets is incorporated to determine the PDF, i.e., larger planets then contribute more to the overall multimodal PDF than smaller planets. The width of each peak w_p was set to such a parameter value that is was ensured that an optimum compromise between a too strong overlap of the Gaussian peaks on the one side and to small peaks on the other was realized. This was ensured with $w_p = 0.15$. The final multimodal PDF, $\rho(\hat{a})$, then represents a sum of Gaussian peaks located at the logarithmized planets' semi-major axis values ($\hat{a}$) and weighted by the individual radius value of the planet (α_i).

To quantify the correlation structure of $\rho(\hat{a})$, the autocorrelation function (ACF) of $\rho(\hat{a})$ was determined according to equations (3) and (4) given in [7]. The ACF properties correspond to the type and grade of the order (short- or long-range) of the input sequence. Finally, the frequency-dependent power spectral density (PSD) of the multimodal PDF $\rho(\hat{a})$ was determined by the periodogram method.

At present, the exact semi-major axis value of the exoplanet TRAPPIST-1h is known only with large uncertainty ($a = 0.063^{+0.027}_{-0.013}$ AU). In an additional analysis, it was tested which a value in the range [0.05, 0.09] AU will maximize the long-range order of the orbital spacing. The maximum was determined by fitting an exponential function to the orbital spacing values while changing the a value for the planet 1h in the range given. The goodness-of-fit was then determined by the coefficient of determination (R^2) and the root-mean-square error (RMSE). The a value that maximized the R^2 and minimized the RMSE was chosen as the one to most likely representing the true value for this exoplanet.
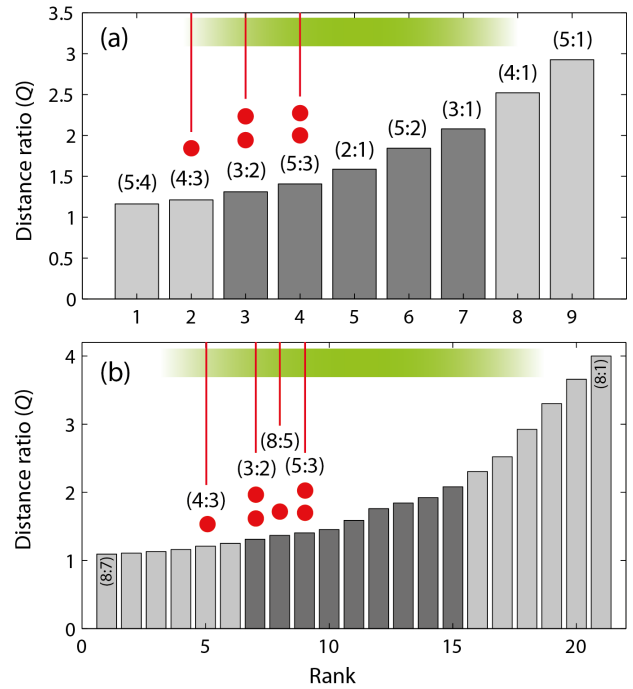

Fig. 1: Distance ratios Q with respect to the rank (given according to the period ratios q). The red dots and vertical lines mark the positions of the exoplanet's orbits according to the distance ratios. (a) Range of distance ratios as used by Aschwanden and McFadden [8]. (b) Range of distance ratios as used in the present study. The green bar marks the interval where it is most likely to find the distances ratios based on empirical data (according to [8]).

2.3 Analysis of harmonic orbital resonances

The methodology based on the recently published *harmonic orbit resonance model* by Aschwanden and McFadden [8] was employed for this analysis. The harmonic orbit resonance model states that the planetary system is best viewed as a self-organisation system where the orbital parameters evolve to attractor states in the sense of harmonical relations (the harmonic orbit resonance). Attracttor states of the orbits are realised when harmonical relations are reached, ensuring stability of the planetary system. The basic idea is that the distance ratios (Q) of semi-major axis values a are (i) not

Harmonic ratio $(H_{i+1} : H_i)$	Distance ratio (Q)	Period ratio (q)	Rank (#)
(8:7)	1.0931	1.1429	1
(8:5)	1.3680	1.6000	8
(8:3)	1.9230	2.6667	14
(8:1)	4.0000	8.0000	21
(7:6)	1.1082	1.1667	2
(7:5)	1.2515	1.4000	6
(7:4)	1.4522	1.7500	10
(7:3)	1.7592	2.3333	12
(7:2)	2.3052	3.5000	16
(7:1)	3.6593	7.0000	20
(6:5)	1.1292	1.2000	3
(6:1)	3.3019	6.0000	19
(5:4)	1.1604	1.2500	4
(5:3)	1.4057	1.6667	9
(5:2)	1.8420	2.5000	13
(5:1)	2.9240	5.0000	18
(4:3)	1.2114	1.3333	5
(4:1)	2.5198	4.0000	17
(3:2)	1.3104	1.5000	7
(3:1)	2.0801	3.0000	15
(2:1)	1.5874	2.0000	11

Table 2: Numerical values of the harmonic ratios, distance ratios and period ratios for all harmonic ratios in the interval $(2 : 1)$ to $(8 : 7)$. The rank of the harmonic ratios is given according to the period ratio values.

constant for a planetary system and (ii) show a quantization whereas only specific values are "allowed" according to

$$Q = \left(\frac{a_{i+1}}{a_i}\right) = \left(\frac{H_{i+1}}{H_i}\right)^{2/3}, \tag{1}$$

with H being harmonic numbers ($H = [1, 2, \ldots, M]$) that form harmonic ratios. Due to Kepler's third law, this equation leads automatically also to quantized orbital period ratios q:

$$q = \left(\frac{P_{i+1}}{P_i}\right) = \left(\frac{a_{i+1}}{a_i}\right)^{3/2} = Q^{3/2}. \tag{1}$$

For $M = 8$ (i.e., $H = [1, 2, \ldots, 8]$), the attractor states are realized by the harmonic ratios $Q = (H_{i+1}/H_i) = (8 : 7)$, $(8 : 5)$, $(8 : 3)$, $(8/1)$, $(7 : 6)$, $(7 : 5)$, $(7 : 3)$, $(7 : 2)$, $(7 : 1)$, $(6 : 5)$, $(6 : 1)$, $(5 : 4)$, $(5 : 3)$, $(5 : 2)$, $(5 : 1)$, $(4 : 3)$, $(4 : 1)$, $(3 : 2)$, $(3 : 1)$ and $(2 : 1)$. The associated numerical values of the distance and period ratios are given in Table 2. When sorted in ascending order of q, the attractor values of the distance ratios Q follow the function as shown in Figure 1. The most dominant ratios in a planetary system, according to Aschwanden and McFadden [8], are marked with a green bar.

3 Results

3.1 Orbital long-range order

As shown in Figure 2(c) the analysis of the semi-major axis values of TRAPPIST-1's planets b-h revealed an exponential function (or a quasi linear one when logarithmized values

were used; Figure 2(d)). The parameter values for the exponential function $f(n) = \alpha \exp^{\beta n}$ were found to be (given as optimal value (95% confidence bound)): $\alpha = 4.086 \times 10^6$ $(3.85 \times 10^6, 4.321 \times 10^6)$, $\beta = 0.5936$ $(0.5398, 0.6475)$.

In an additional analysis, it was investigated if the fit with an exponential function related to the Titius-Bode law [12] in the form $f(n) = \alpha + \beta 2^n$ was better or worse at describing the data than the exponential function of type $f(n) = \alpha \exp^{\beta n}$ (with α and β free parameters), as also used by Naficy et al. [11] to describe the planetray orbit scaling. It was found (see Figures 4(a) and (b)) that the second exponential model fitted the data better than the first one (coefficient of determination (R^2: 0.9921 and 0.9944, respectively).

Figure 2(e) shows the calculated multimodal PDF. The ACF and the power spectrum are depicted in Figures 2(f) and 2(g), respectively. A clear peak of the spectrum of the multimodal PDF is evident with a center frequency of 3.47 $1/\hat{a}$, corresponding to a an orbital spacing regularity with a spacing of 0.288.

3.2 Prediction of the TRAPPIST-1h exoplanet position

Figure 3 depicts the results of the analysis investigating how the orbital position of the TRAPPIST-1h exoplanet has an effect on the long-range order. The "optimal" position (i.e., maximizing R^2 and minimizing RMSE) were found to be in the range $a = [0.060, 0.061$ AU].

3.3 Harmonic orbital resonances

The analysis with the *harmonic orbit resonance model* by Aschwanden and McFadden [8] revelaed that all exoplanets of the TRAPPIST-1 system occupy orbitals that are attractor states according to the harmonic orbital resonance model (see Figure 4(c)). The harmonic ratios describing the planetary system are found to be: $(H_{i+1}/H_i) = (4 : 3)$, $(3 : 2)$, $(8 : 5)$, and $(5 : 3)$. The ratios $(3 : 2)$, $(8 : 5)$, and $(5 : 3)$ are in the interval where the most dominant ratios are being expected according to Aschwanden and McFadden [8]. The ratios $(4 : 3)$ is at the border of this interval (see Figure 1).

4 Discussion and conclusion

The following conclusions can be drawn from the analysis conducted in the present study:

(i) The orbitals of the exoplanets of the TRAPPIST-1 planetary system exhibit a long-range order. This property is cleary visible in the linear periodicity of the multimodal PDF when logarithmizing the distances between the planets. The single peak in the power spectrum quantifies this characteristic.

(ii) The orbital postition of the TRAPPIST-1h exoplanet is most likely in the range of $a = [0.060, 0.061$ AU].

(iii) All exoplanets of the TRAPPIST-1 system occupy orbitals that are attractor states according to the harmonic orbital resonance model.
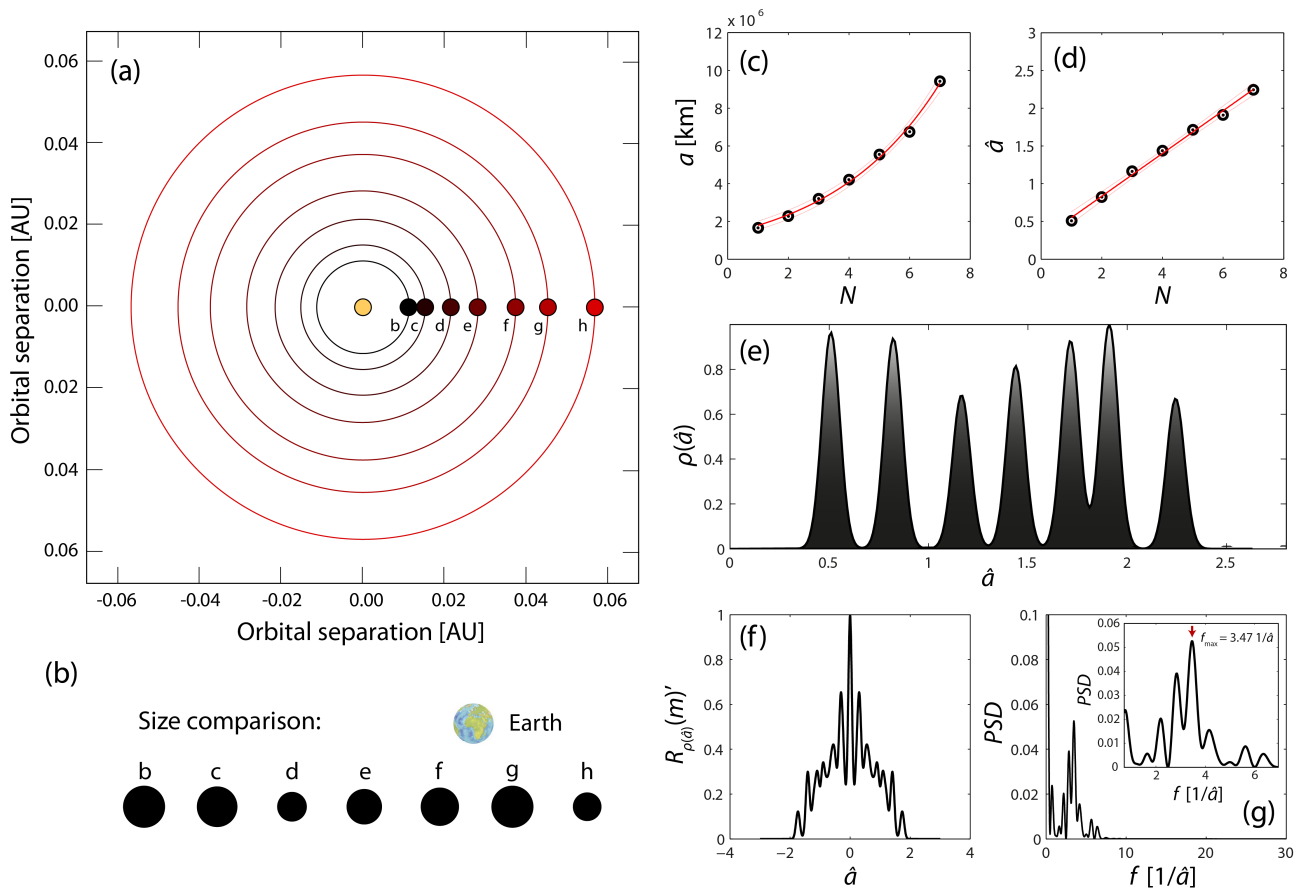
Fig. 2: (a) Diagram with the orbits of the exoplanets of TRAPPIST-1. (b) Comparison of the exoplanets' sizes with respect to the size of the Earth. (c, d) Semi-major axis values with respect to the rank (n), plotted in linear and logarithmic space, respectively. (e) Multimodal PDF of the seven exoplanets. (f) ACF and (f) power spectrum of the multimodal PDF
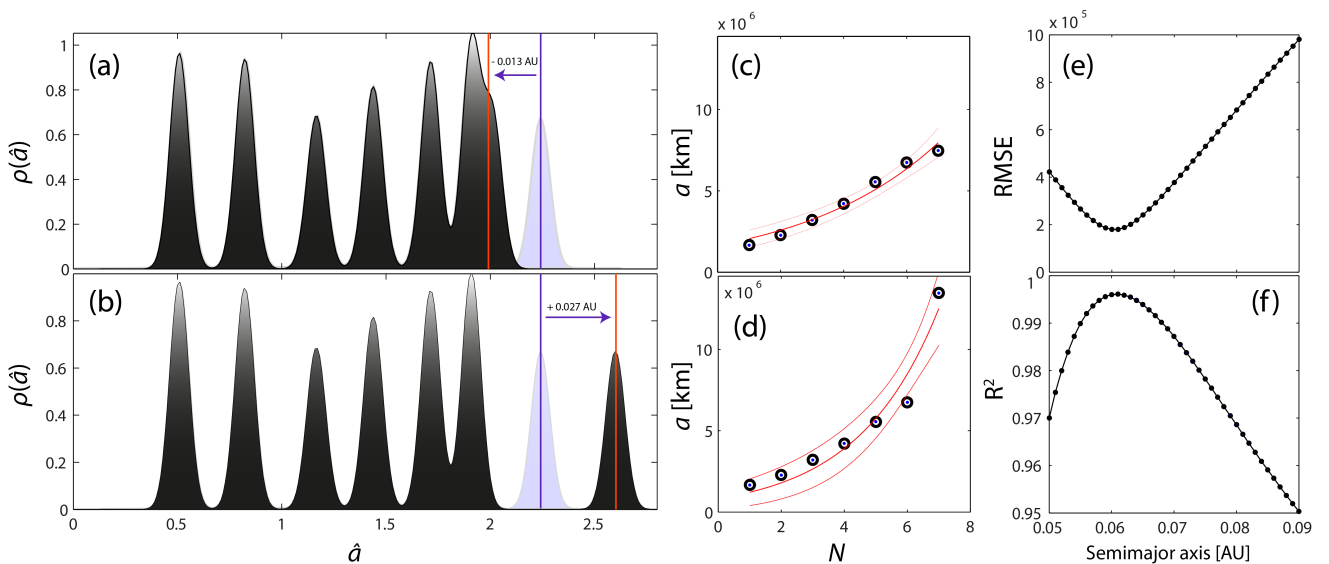

Fig. 3: (a, b) Multimodal PDFs $\rho(\hat{a})$ with different positions of the exoplanet TRAPPIST-1h. The corresponding scaling functions (a vs. rank (n)) are shown in (c) and (d), respectively. (e) R^2 vs. a. (f) RMSE vs. a.
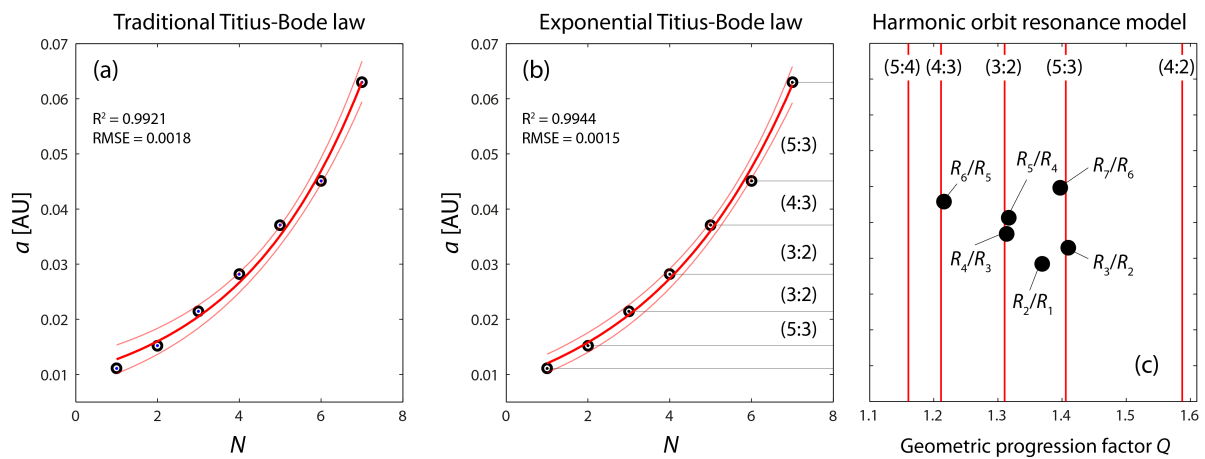
Fig. 4: Fitting of the semi-major axis values with two different types of exponential functions, i.e., (a) $f(n) = \alpha + \beta \, 2^n$ and (b) $f(n) = \alpha \exp^{\beta n}$. (c) Predicitons of the orbital positions according to the harmonic orbit resonance model, and the corresponding values of the TRAPPIST-1 exoplanetary system.

What is the physical mechanism causing this long-range order and the harmonic orbital resonances? A review of different approaches and models related to this question can be found in my previously published paper [7] as well as one recently published by Aschwanden and McFadden [8]. In my opinion, the most promising and interesting aproaches are those based on plasma physics [13–17], the concept of macroscopic quantization due to finite gravitational propagation speed [18], and the view that the solar system is a self-organising system with attractor states leading to harmonic orbit resonances [8].

In conclusion, the present analysis of the extrasolar planetary system TRAPPIST-1 reveals that the semi-major axis values of the planets follow (i) a long-range order and (ii) a quantization in accordance with the harmonic orbital resonance model. Furthermore, the analysis predicts that the exact position of the exoplanet TRAPPIST-1h is in the range of $a = [0.060, 0.061 \text{ AU}]$, slightly less then the determined mean semi-major axis value of 0.063 AU given by Gillon et al. [1].

References

1. Gillon M., Triaud A.H.M., Demory B.-O., Jehin E., Agol E., et al. Seven temperate terrestrial planets around the nearby ultracool dwarf star TRAPPIST-1. *Nature*, 2017, v. 542, 456–460.

2. Gillon M., Jehin E., Lederer S.M., Delrez L., et al. Temperate Earth-sized planets transiting a nearby ultracool dwarf star. *Nature*, 2016, v. 533, 221–224.

3. Mills S.M., Fabrycky D.C., Migaszewski C., Ford E.B., et al. A resonant chain of four transiting, sub-Neptune planets. *Nature*, 2016, v. 533, 509–512.

4. MacDonald M.G., Rogozzine D., Fabrycky D.C., Ford E.B., Holman M.J., et al. A dynamical analysis of the Kepler-80 system of five transiting planets. *The Astronomical Journal*, 2016, v. 152 (4), 105.

5. Man Hoi L. and Peale S.J. Dynamics and origin of the 2:1 orbital resonances of the GJ 876 planets. *The Astrophysical Journal*, 2002, v. 567 (1), 596–609.

6. Goździewski K. and Maciejewski A.J. Dynamical analysis of the orbital parameters of the HD 82943 planetary system. *The Astrophysical Journal*, 2001, v. 563 (1), L81.

7. Scholkmann F. A prediction of an additional planet of the extrasolar planetary system Kepler-62 based on the planetary distances' long-range order. *Progress in Physics*, 2013, v. 4, 85–89.

8. Aschwanden M.J. and McFadden L.A. Harmonic resonances of planet and moon orbits – From the Titius-Bode law to self-organizing systems *arXiv:1701.08181 [astro-ph.EP].*

9. Bohr J. and Olsen K. Long-range order between the planets in the Solar system. *Monthly Notices of the Royal Astronomical Society*, 2010, v. 403, L59–L63.

10. Olsen K. and Bohr J. Pair-correlation analysis of HD 10180 reveals a possible planetary orbit at about 0.92 AU. 2010, arXiv: astro-ph.EP/1009.5507.

11. Naficy K., Ayubinia A. and Saeedi M. Exponential law as a more comp atible model to describe orbits of planetary systems. *Iranian Journal of Physics Research*, 2012, v. 12 (3), 25–31.

12. Jaki S. L. The early history of the Titius-Bode law. *American Journal of Physics*, 1972, v. 40 (7), 1014–1023

13. Wells D. R. Was the Titius-Bode series dictated by the minimum energy states of the generic solar plasma? *IEEE Transactions on Plasma Science*, 1990, v. 19 (1), 73–76.

14. Wells D. R. Titius-Bode and the helicity connection: a quantized field theory of protostar formation. *IEEE Transactions on Plasma Science*, 1989, v. 14 (6), 865–873.

15. Wells D. R. Quantization effects in the plasma universe. *IEEE Transactions on Plasma Science*, 1989, v. 17 (2), 270–281.

16. Wells D. R. Unification of gravitational, electrical, and strong forces by a virtual plasma theory. *IEEE Transactions on Plasma Science*, 1992, v. 20 (6), 939–943.

17. Livadiotis G., McComas D.J. Evidence of large-scale quantization in space plasmas. *Entropy*, 2013, v. 15, 1118–1134.

18. Giné J. On the origin of the gravitational quantization: The Titius–Bode law. *Chaos, Solitons & Fractals*, 2007, v. 32 (2), 362–369.